Supplementary Figure 1

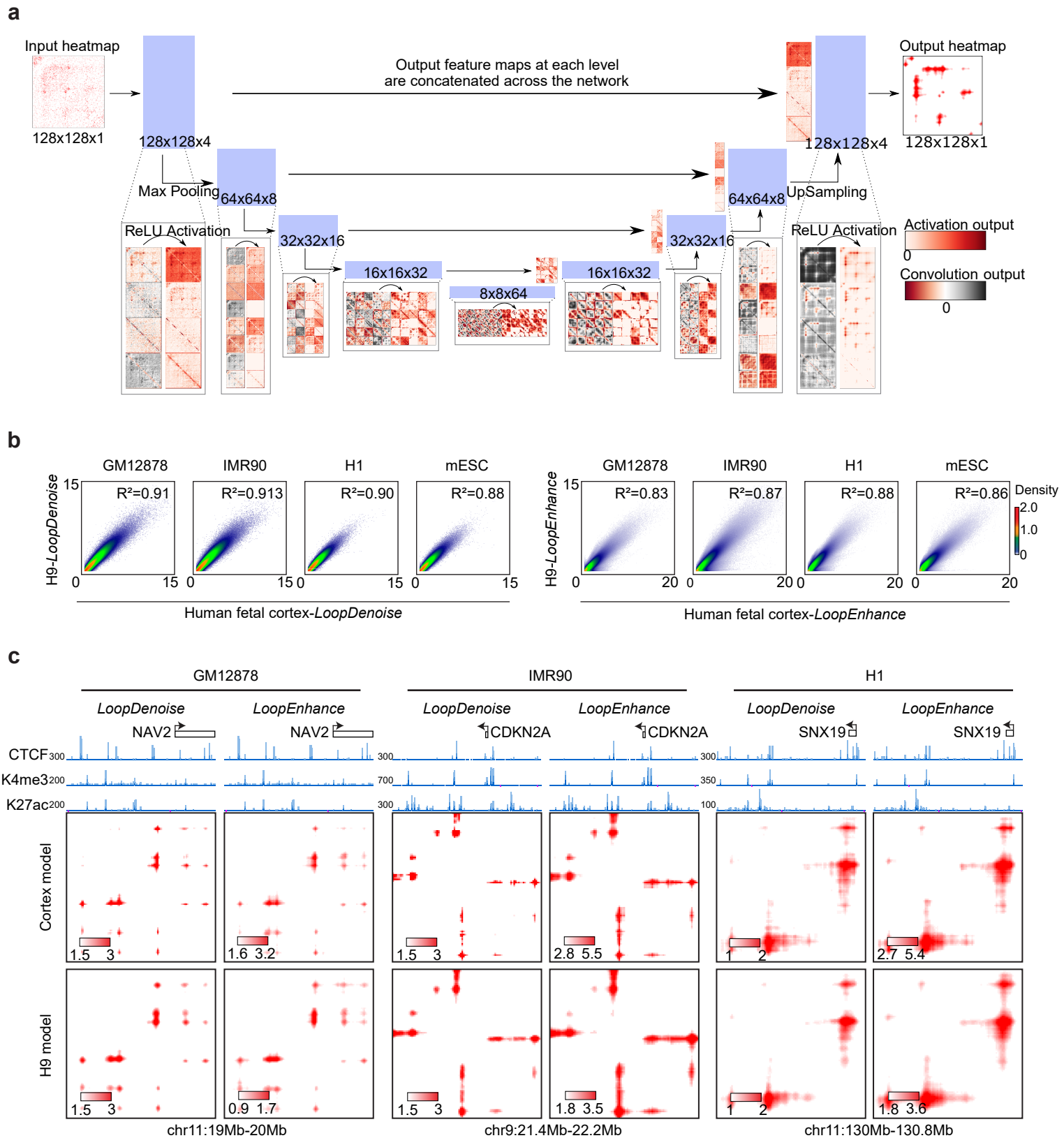

Supplementary Fig.1 *LoopDenoise* training procedure, performance, and visualization.

a, Detailed *LoopDenoise* convolutional autoencoder model architecture showing five convolution layers, two in the encoding path using eight 13x13 filters, two transpose convolution layers in the decoding path using eight 2x2 filters, and one final convolution layer using a single 13x13 filter. The matrices dimensions of each layer output were also shown. Each layer is visualized by the filters used, the output of convolving the input with this filter, the result of applying *ReLU* activation, and the result of max pooling. The convolution operation is denoted by *. **b,** Venn diagram showing the reproducible loop pixels between three human fetal brain replicates. The table showing the number of overlapped pixels between significant pixels in the pooled data and each part of pixels shown in the Venn diagram. The pixels that are significant in both pooled data and at least one of the three replicates are the training target in the *LoopDenoise* model. The significance of loop pixels come from the negative binomial test wrapped in HiCorr package. **c,** Pairwise reproducibility at pixel level (defined as the fraction of common ones when calling the same number of loop pixels from two datasets) between biological replicates of human fetal cortex Hi-C data, when the same numbers of the loop pixels were called. **d**, The heatmap examples from 8 locus in three human fetal brain replicates, and *LoopDenoise* output showing more reproducible contact patterns. The maximum color scale value is labeled on the bottom left of each heatmap.

Supplementary Figure 2

a

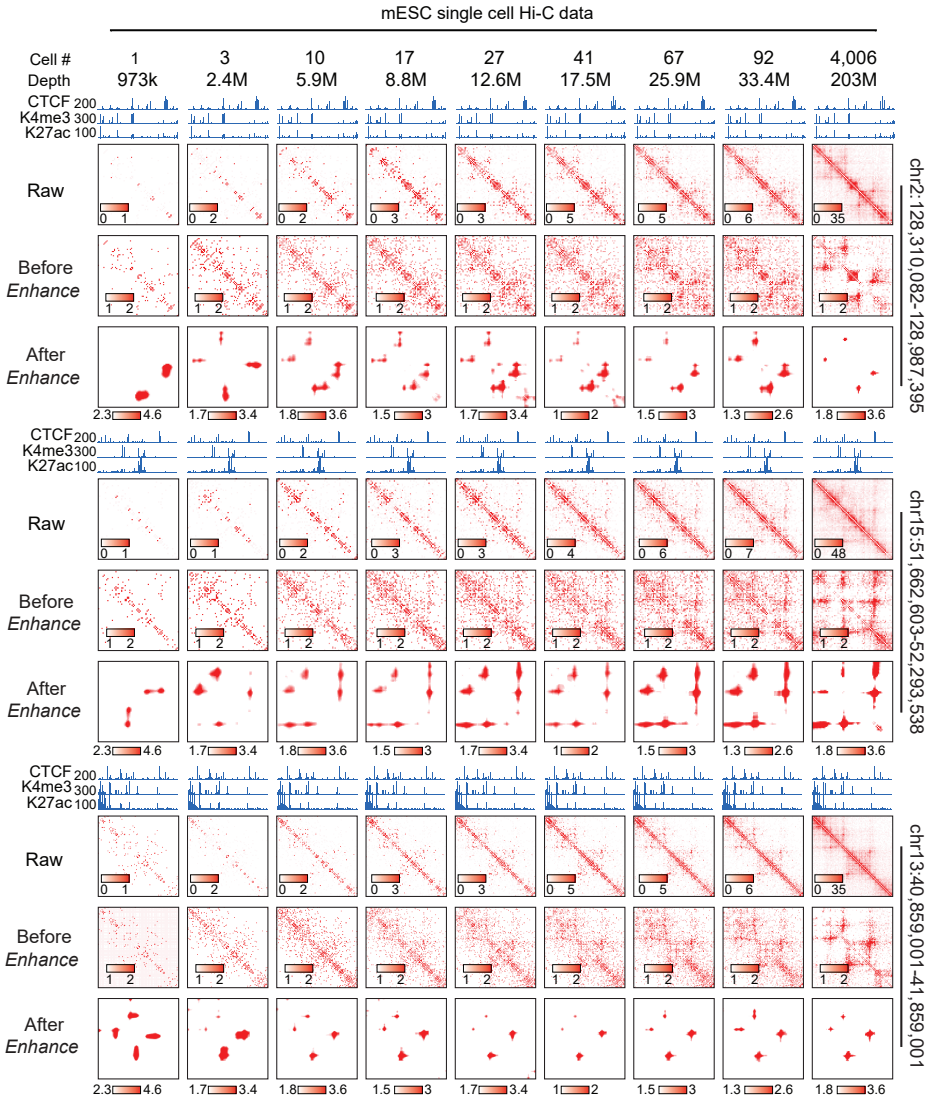

b

Tables: Coverage of 77,393 mESC pcHi-C loops with scHi-C data

When calling 300K loop pixels from scHi-C

Cell #	Depth	short PP (<=100kb) n=10,632	long PP (>100kb) n=18,882	short PO (<=100kb) n=27,216	long PO (>100kb) n=38,073
3	2.4M	709 (6.7%)	2,134 (11.3%)	2,253 (8.3%)	8,840 (23.2%)
10	5.9M	1,263 (11.9%)	2,118 (11.2%)	4,220 (15.5%)	9,831 (25.8%)
17	8.8M	1,667 (15.7%)	2,231 (11.8%)	5,424 (19.9%)	10,064 (26.4%)
27	12.6M	1,365 (12.8%)	1,938 (10.3%)	4,382 (16.1%)	9,369 (24.6%)
41	17.5M	1,214 (11.4%)	1,582 (8.4%)	4,036 (14.8%)	7,967 (20.9%)
67	25.9M	952 (9.0%)	1,560 (8.3%)	3,450 (12.7%)	8,596 (22.6%)
92	33.4M	1,063 (10.0%)	2,230 (11.8%)	3,935 (14.5%)	11,147 (29.3%)
4,006 *	203M	259 (2.4%)	1,050 (5.6%)	1,145 (4.2%)	7,792 (20.5%)

* The 4,006-cell data were analyzed with HiCorr only without enhancement

When calling 500K loop pixels from scHi-C

Cell #	Depth	short PP (<=100kb) n=10,632	long PP (>100kb) n=18,882	short PO (<=100kb) n=27,216	long PO (>100kb) n=38,073
3	2.4M	1,305 (12.3%)	3,038 (16.1%)	3,904 (14.3%)	11,381 (29.9%)
10	5.9M	1,894 (17.8%)	2,843 (15.1%)	5,865 (21.5%)	12,153 (31.9%)
17	8.8M	2,429 (22.8%)	2,930 (15.5%)	7,328 (26.9%)	12,097 (31.8%)
27	12.6M	1,905 (17.9%)	2,526 (13.4%)	5,818 (21.4%)	11,343 (29.8%)
41	17.5M	1,675 (15.8%)	2,053 (10.9%)	5,124 (18.8%)	9,598 (25.2%)
67	25.9M	1,295 (12.2%)	2,104 (11.1%)	4,363 (16.0%)	10,225 (26.9%)
92	33.4M	1,420 (13.4%)	2,862 (15.2%)	5,007 (18.4%)	13,280 (34.9%)
4,006 *	203M	369 (3.5%)	1,416 (7.5%)	1,535 (5.6%)	9,447 (24.8%)

* The 4,006-cell data were analyzed with HiCorr only without enhancement

When calling 1M loop pixels from scHi-C

Cell #	Depth	short PP (<=100kb) n=10,632	long PP (>100kb) n=18,882	short PO (<=100kb) n=27,216	long PO (>100kb) n=38,073
3	2.4M	2,644 (24.9%)	4,548 (24.1%)	7,689 (28.3%)	15,583 (40.9%)
10	5.9M	3,089 (29.1%)	4,148 (22.0%)	9,001 (33.1%)	15,671 (41.2%)
17	8.8M	3,708 (34.9%)	4,089 (21.7%)	10,427 (38.3%)	15,321 (40.2%)
27	12.6M	2,909 (27.4%)	3,572 (18.9%)	8,250 (30.3%)	14,281 (37.5%)
41	17.5M	2,501 (23.5%)	2,973 (15.7%)	7,156 (26.3%)	12,474 (32.8%)
67	25.9M	1,969 (18.5%)	3,078 (16.3%)	6,104 (22.4%)	13,121 (34.5%)
92	33.4M	2,162 (20.3%)	4,103 (21.7%)	6,882 (25.3%)	16,631 (43.7%)
4,006 *	203M	567 (5.3%)	2,088 (11.1%)	2,298 (8.4%)	11,995 (31.5%)

* The 4,006-cell data were analyzed with HiCorr only without enhancement

Supplementary Fig.2 *LoopDenoise* generalization across cell types and species.

a, Ten heatmap examples in GM12878, the highlight row is the output from *LoopDenoise*. The maximum color scale value is labeled on the bottom left of each heatmap. **b**, The distance distribution of top 300K pixels in H1(hESC), GM12878, IMR90 and mESC. All data are presented as means ± SEM from triplicate experiments. **c**, The number of loops pixels with at least one anchor overlapped with ChIP-seq peaks out of top 300K pixels. **d**, Density plots show the distribution of distances between loop anchors (top 100K loop pixels used) and their nearest ChIP-seq peaks in GM12878, IMR90, H1(hESC) and mESC. **e**, The heatmap examples of six loci with known long-range gene regulation. The maximum color scale value is labeled on the bottom left of each heatmap.

Supplementary Methods

Reproducibility between replicates

We took variable numbers of top loops identified from datasets before and after *LoopDenoise* or *LoopEnhance*. For each certain number of top loops N, the percentage of the overlapping loops between $rep1$ and $rep2$ is the reproducibility.

$$Reproducibility = \frac{N_{rep1 \cap rep2}}{N}$$

Distance analysis between ChIP-seq peak and Hi-C loops

We used macs2 (v2.2.7.1) (default parameter) to call peaks for ChIP-seq data in bed format. For each bias corrected Hi-C dataset, we ranked the ratio before or after denoise and took the top loops. The distance distribution between each anchor region involved in the top loops and its closest ChIP-seq peak was shown by 3D-density plots. The p-values were calculated by *Wilcox test*. The 3D-density plots were generated by performing multivariate kernel density estimation on the set of all distances to the closest ChIP-seq peak for the two anchors participating in each loop.

Dynamic loop identification between CP and GZ

All the loops (ratio>=2) from CP and GZ before and after *LoopDenoise* were taken to plot the scatter plot and fed to the linear model (GZ~CP). We took the union of top 500 loops ranked by residuals from datasets before and after *LoopDenoise*. The processed ATAC-seq bed files were downloaded and merged.

Compare *DeepLoop* loop callings to pcHi-C

To validate the loops identified by *LoopDenoise* or *LoopEnhance* with loops identified by Promoter Capture Hi-C (pcHi-C), we used a confusion matrix to analyze precision, recall, and a ROC curve. To do this, we treated the significant (*p-value* < *0.01*) pcHi-C loops as positive labels and all other pcHi-C loops as negative labels. When analyzing the PP (promoter-promoter) loops, we only considered the Hi-C loops with two ends containing promoters tested in pcHi-C. When analyzing the PO (promoter-other region) loops, we considered the loops with at least one end overlapping with promoter tested. The selected loops were ranked by ratio values. We treated the top *k* loops as positive classifications and the rest of the values as negative classifications. The true positives were the common loops between the significant pcHi-C loops and the top *k* loops we took. False positives were the common loops between the insignificant pcHi-C loops and the top *k* loops we took. False negatives were the loops not in the top *k* loops but were significant in pcHi-C. True negatives were the common loops between the insignificant pcHi-C loops and the unselected loops. We varied *k* from zero up to the

total number of loops we were considering. This allowed us to measure the true positive rate and false positive rate from a purely negative class classifier up to a purely positive class classifier and every point in between to plot a ROC curve. For PP analysis, we used an interval of 1000 loops when varying *k,* and for PO we use an interval of 5000. mESC pcHi-C loops called by CHICAGO are in Supplementary Table 3.

Compare *DeepLoop* loop callings to ChIA-PET and HiChIP

The loop callings from ChIA-PET and HiChIP experiments in GM12878 were downloaded from the original study[13,14] (Supplementary Table 1). We grouped loops in these 5 experiments by the number of sharing loops among them. Then we summarized the overlapping loops between the grouped loops and the top500K and top1M loops identified from down sampled 50M Hi-C datasets before and after *LoopEnhance*, and high-depth data (~380M) before *LoopDenoise* (shown by pie charts in Figure 2*f*).

Compare the performance of *DeepLoop* to published Hi-C data analytical pipelines

HiCPlus, *HiCNN2*[15], and *SRHiC*[16] studies all provide enhance models trained by 1/16 down sampled 4-cutter (*MboI*) GM12878 Hi-C dataset. To avoid the difference of training these models by our own, we directly used these models downloaded from their original studies. We chose a *LoopEnhance* model trained by 50M down sampled 6-cutter (*HindIII*) human fetal cortex data for the comparison. For 4-cutter Hi-C datasets, we chose a 94M down-sampled dataset (1/16 of the original depth) used in *HiCPlus*, *HiCNN2*, and *SRHiC* studies, and the 1.35 billion full-depth as reference. For 6-cutter Hi-C datasets, we chose a 50M down-sampled dataset and the 380M full-depth as reference. The conventional pipeline for Hi-C data processing involves KR/ICE normalization, we further added distance correction step for a fair comparison to *HiCorr*. The *HiCPlus*, *HiCNN2*, and *SRHiC* models were trained on raw data, the pipelines for all three models are to enhance raw contact matrix first and following KR/ICE normalization and we further added another column of heatmaps examples by correcting distance bias. The *LoopEnhance* models were trained on *HiCorr* normalized contact matrix, so the *DeepLoop* pipeline requires *HiCorr* normalization first and then enhanced. In Supplementary Figure. 5, *DeepLoop* pipelines reveals cleaner contact patterns matched with ChIP-seq peak signals in different enzyme based Hi-C datasets.

Compare DeepLoop loop callings to HiCCUPS loop callings from Micro-C

As we mentioned in “Micro-C” data processing section, we used Juicebox to convert 5kb bin contact pairs to “*Micro-C*.hic” format, and then we ran HICCUPS at 5kb resolution for all the chromosomes as follows:

java -jar juicer_ml_tools.jar hiccups –cpu -m 500 -r 5000 -c 1,2,3,4,5,6,7,8,9,10,11,12,13,14,15,16,17,18,19,20,21,22,X,Y -k KR --threads 12 MicroC.hic all_hiccups_loops

We took file "merged_loops.bedpe" as the loop calls to compare with other datasets.

HiCorr includes distance correction step, therefore, for a fair comparison, we calculated "KR-ratio", which is KR normalization and distance correction, for enhanced low-depth output of *HiCPlus*, *HiCNN2*, and *SRHiC.* And the low and high depth "KR-ratio" were also included as the reference. For each dataset, we ranked contact pairs by their enhanced or normalized value and varied the top ranked contact pairs to calculate TPR and RPR comparing to the ground truth data, microC HiCCUPS loop calls. Then we used a series of TPR and FPR values to plot ROC curves.

Compare Hi-C datasets with different restriction enzymes and Micro-C

The *DeepLoop* output contacts are 5kb anchor based, which were converted to 5kb bin pairs for comparison across restriction enzymes or methods. The *Spearman* correlation was calculated for measurement of consistency between Hi-C datasets and Micro-C dataset.

Compare scHi-C and bulk Hi-C

ROC curves

We measured true positive rate and false positive as the following:

$$TPR = \frac{TP}{TP\ +\ FN}$$

$$FPR = \frac{FP}{FP\ +\ TN}$$

Then we plot the true positive rate versus the false positive rate to obtain a Receiver Operating Characteristic (ROC) curve. The area under the ROC curve (AUC) is a common metric used to validate model performance. To compute this value, we considered a set of discrete points in the ROC curve and performed a trapezoidal sum to approximate the area under the curve. This is an approximation of the following integral:

$$\int_0^1 f(x)dx \approx \sum_{k=0}^{N} \Delta x_k \frac{f(x_{k-1}) + f(x_k)}{2}$$

We took the top 300K loops from bulk Hi-C data after *LoopDenoise* as ground truth and took the variable number of top loops from single-cell Hi-C datasets before and after *LoopEnhance* to plot the ROC curve, which is the same strategy as described above.

Accuracy

We took the top 300,000 loops from high-depth data after *LoopDenoise* as ground truth loops T and took the variable numbers of top loops i from the datasets before and after *LoopDenoise* or *LoopEnhance*. For each certain number of top loops N_i, the fraction between the number of loops overlapped with ground truth and the number of

top loops is the accuracy.

$$Accuracy = \frac{N_i \cap T}{i} \ , i \in (1000, 3000, 5000, 100000, 200000, 300000)$$

Chromatin Loop-level tissue cluster

We took the top 100K loops from 14 tissue datasets before and after *LoopEnhance* and calculated the fraction of overlapped loops between every two tissues. Then we used corrplot (v0.92) function to generate hierarchical clustering heatmap.

Human prefrontal cortex sn-m3C-seq methylation clustering

We compute CG methylation levels (mCG) for non-overlapping 100kb bins in each of the 4,238 cells as outlined in the *sn-m3C-seq* paper. The same filtering strategy is also applied by selecting only the bins with at least 20 CG reads in at least 90% of the cells. We then use Linear Discriminant Analysis (LDA) to perform a linear dimensionality reduction step on the cell-bin matrix. The first 50 dimensions of the LDA embedding were visualized with t-SNE.

Identification of escape loops and repressive loops

In the top300K loop pixels of maternal and paternal loops, 3,605 loops are on chrX. The loops that are in the top300K ranked in both maternal and paternal were defined as “escape loops”. The loops that are only identified in maternal (active allele) but not in paternal (inactive allele) were identified as “repressive loops”.

Identification of SVs by loops

We applied *HiCorr* and 50M *LoopEnhance* models on the two alleles datasets from 4-cutter GM12878 and took the union of the top 300K loops from each allele. The 10-fold was used to define the extremely specific loops between two alleles. We merged these loops with distance less than 50kb, and found they mainly locate in four loci. We extended 100kb upstream and downstream of escape gene promoters to overlap with loop pixels (Supplementary Table 4).

Fix Inversion Hi-C

To fix two inversion loci identified from extremely specific loops, we estimated the breakpoints considering the Hi-C heatmap pattern and location reported in other studies. We reverted the inversion loci before applying *HiCorr* and flipped the region when the *HiCorr* and *DeepLoop* were done.

Motif analysis on specific loops

The 769 human motifs (*.meme* format) was downloaded from HOCOMOCO (v11) motif

database[17] (https://hocomoco11.autosome.ru/downloads_v11). The 51bp (25bp up/down) long sequence centered around SNPs in allele-specific loop anchors from two allele genomes were treated as loop-positive sequence and loop-negative sequence. We used fimo (v4.11.2)[18] to scan each motif in the database on the two sequence datasets. Considering the bias of motif length, we chose "*q-value<0.3"* as the cutoff to summarize the frequency of each motif on the loop-positive and loop-negative sequence sets. Then, the *fisher. Exact test* was performed to measure the motif enrichment in two sets, the motifs with *"p-value<=0.05"* were defined as significantly enriched motifs in loop-positive sequence (Supplementary Table 5).

Identification of SNPs that impact chromatin loops

In the 20,772 CTCF peaks with CTCF motif, 809 CTCF peaks contain SNPs. We further filtered these peaks by overlapping the top 300K loops identified in two alleles. Two-fold was chosen to define specific binding peaks and specific loops between two alleles. The consistently specific peaks refer to the peaks with specific binding and specific loops (e.g., maternal-specific binding peaks overlap maternal-specific loops) (Supplementary Table 6).

References

1. Durand, N.C. *et al.* Juicer Provides a One-Click System for Analyzing Loop-Resolution Hi-C Experiments. *Cell Syst* **3**, 95-8 (2016).
2. Nagano, T. *et al.* Cell-cycle dynamics of chromosomal organization at single-cell resolution. *Nature* **547**, 61-67 (2017).
3. Kent, W.J. *et al.* The human genome browser at UCSC. *Genome Res* **12**, 996-1006 (2002).
4. Quinlan, A.R. & Hall, I.M. BEDTools: a flexible suite of utilities for comparing genomic features. *Bioinformatics* **26**, 841-2 (2010).
5. Siva, N. 1000 Genomes project. *Nat Biotechnol* **26**, 256 (2008).
6. Rao, S.S. *et al.* A 3D map of the human genome at kilobase resolution reveals principles of chromatin looping. *Cell* **159**, 1665-80 (2014).
7. Langmead, B. & Salzberg, S.L. Fast gapped-read alignment with Bowtie 2. *Nat Methods* **9**, 357-9 (2012).
8. Krueger, F. & Andrews, S.R. SNPsplit: Allele-specific splitting of alignments between genomes with known SNP genotypes. *F1000Res* **5**, 1479 (2016).
9. Zhang, Y. *et al.* Model-based analysis of ChIP-Seq (MACS). *Genome Biol* **9**, R137 (2008).
10. Kim, D., Langmead, B. & Salzberg, S.L. HISAT: a fast spliced aligner with low memory requirements. *Nat Methods* **12**, 357-60 (2015).
11. Liao, Y., Smyth, G.K. & Shi, W. featureCounts: an efficient general purpose program for assigning sequence reads to genomic features. *Bioinformatics* **30**, 923-30 (2014).
12. Krijger, P.H.L., Geeven, G., Bianchi, V., Hilvering, C.R.E. & de Laat, W. 4C-seq

from beginning to end: A detailed protocol for sample preparation and data analysis. *Methods* **170**, 17-32 (2020).
13. Heidari, N. *et al.* Genome-wide map of regulatory interactions in the human genome. *Genome Res* **24**, 1905-17 (2014).
14. Tang, Z. *et al.* CTCF-Mediated Human 3D Genome Architecture Reveals Chromatin Topology for Transcription. *Cell* **163**, 1611-27 (2015).
15. Liu, T. & Wang, Z. HiCNN2: Enhancing the Resolution of Hi-C Data Using an Ensemble of Convolutional Neural Networks. *Genes (Basel)* **10**(2019).
16. Li, Z. & Dai, Z. SRHiC: A Deep Learning Model to Enhance the Resolution of Hi-C Data. *Front Genet* **11**, 353 (2020).
17. Kulakovskiy, I.V. *et al.* HOCOMOCO: towards a complete collection of transcription factor binding models for human and mouse via large-scale ChIP-Seq analysis. *Nucleic Acids Res* **46**, D252-D259 (2018).
18. Bailey, T.L., Johnson, J., Grant, C.E. & Noble, W.S. The MEME Suite. *Nucleic Acids Res* **43**, W39-49 (2015).